A Computational Study of Methyl α-D-Arabinofuranoside: Effect of Ring Conformation on Structural Parameters and Energy Profile

Matthew T. Gordon, Todd L. Lowary,* and Christopher M. Hadad*

Contribution from the Department of Chemistry, The Ohio State University, Columbus, Ohio 43210

Received May 7, 1999. Revised Manuscript Received August 19, 1999

Abstract: Ab initio molecular orbital calculations at the HF/6-31G* level of theory and density functional theory calculations at the B3LYP/6-31G* level have been carried out on methyl α-D-arabinofuranoside (**1**). All 10 possible envelope forms were constructed and minimized, providing a partial energy surface which identified ^{3}E as the lowest energy north conformer and, depending on the level of theory used, either ^{2}E or E_1 as the southern hemisphere minimum. The southern conformation was the global minimum regardless of the level of theory. The energy profile identifies pseudorotation through the eastern pathway as the most favorable. Pseudorotation through the west is higher in energy and similar to inversion through the planar species. The dependence of structural parameters (i.e., bond distances, bond angles, dihedral angles, and interatomic distances) on the ring conformation have been determined. Energy profiles based on additional electron correlation and extended basis sets with the HF/6-31G* geometries are presented and provide qualitatively similar results to the B3LYP/6-31G* profile.

Introduction

A number of bacteria, fungi, and parasites synthesize oligosaccharides containing furanosyl residues, and these glycans are often critical components of the protective cell wall structure found external to the cytoplasmic membrane of these organisms.[1−3] Of particular interest to this work are the two major polysaccharides present in the cell wall of mycobacteria, including the human pathogens *Mycobacterium tuberculosis* and *M. leprae*.[1] These polymers, an arabinogalactan (AG) and a lipoarabinomannan (LAM), play important roles in the survival and pathogenicity of these species and are composed largely of arabinofuranose and galactofuranose residues. One of the major structural motifs in these polysaccharides is the hexasaccharide shown in Scheme 1. This structure is found at the nonreducing end of both polymers and in the AG, it serves as a scaffold for the attachment of mycolic acids, long-chain branched fatty acids that are characteristic to mycobacteria and related *Actinomycetes*.

It is unknown why mycobacteria have evolved to synthesize polysaccharides containing the thermodynamically less stable ring forms of these sugars. One postulate put forward[4] is that the predicted greater inherent flexibility of these glycans relative to those containing pyranose residues allows the tight, side-by-side packing of the mycolic acids attached to the AG. The resulting near-crystalline array of lipids presents a thick, hydrophobic facade that both protects the organism from the immune system of the host and blocks the passage of antibiotics across the cell membrane. This hypothesis is, however, untested,

Scheme 1

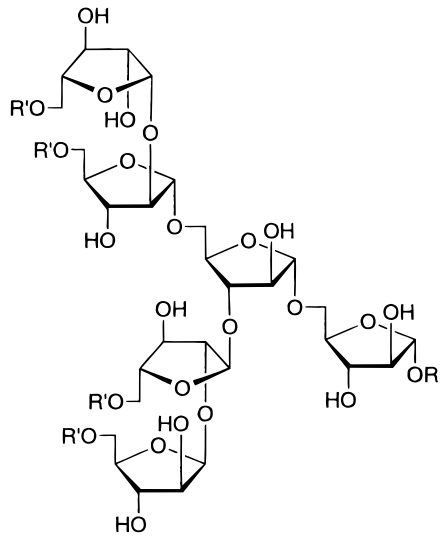

AG: R = arabinogalactan; R' = mycolic acids
LAM: R = arabinomannan; R' = H

and a more detailed understanding of the conformational preferences of furanose oligosaccharides is required before this question can be addressed.

Central to the problem of elucidating the conformational preferences of oligo- or polyfuranosides is an understanding of the flexibility of the constituent monosaccharide residues. Unlike their pyranose brethren, which generally exist in well-defined chair conformations in solution,[5] furanose rings are flexible species that can adopt a multitude of twist (T) and envelope (E) conformations of often comparable energies.[6] The standard model used to describe furanose ring conformation makes use

(1) Brennan, P. J.; Nikaido, H. *Annu. Rev. Biochem.* **1995**, *64*, 29−63.
(2) (a) Gerold, P.; Eckert, V.; Schwarz, R. T. *Trends Glycosci. Glycotechnol.* **1996**, *8*, 265. (b) de Lederkremer, R. M.; Colli, W. *Glycobiology* **1995**, *5*, 547.
(3) (a) Unkefer, C. J.; Gander, J. *J. Biol. Chem.* **1990**, *265*, 685. (b) Mendonça-Previato, L.; Gorin, P. A. J. *Infect. Immun.* **1980**, *29*, 934. (c). Groisman, J. F.; de Lederkremer, R. M. *Eur. J. Biochem.* **1987**, *165*, 327.
(4) Connell, N. D.; Nikaido H. Membrane Permeability and Transport in Mycobacterium tuberculosis. In *Tuberculosis: Pathogenesis, Prevention, and Control;* American Society for Microbiology Press: Washington, DC, 1994; pp 333−352.
(5) (a) Peters, T.; Pinto, B. M. *Curr. Opin. Struct. Biol.* **1996**, *6*, 710. (b) Homans, S. Conformational Studies of Oligosaccharides: NMR and Modeling Studies. In *Molecular Glycobiology;* Fukuda, M., Hindsgaul, O., Eds.; IRL Press: Oxford, 1994; pp 230−257.

10.1021/ja9915091 CCC: $18.00
Published on Web 10/01/1999

Scheme 2

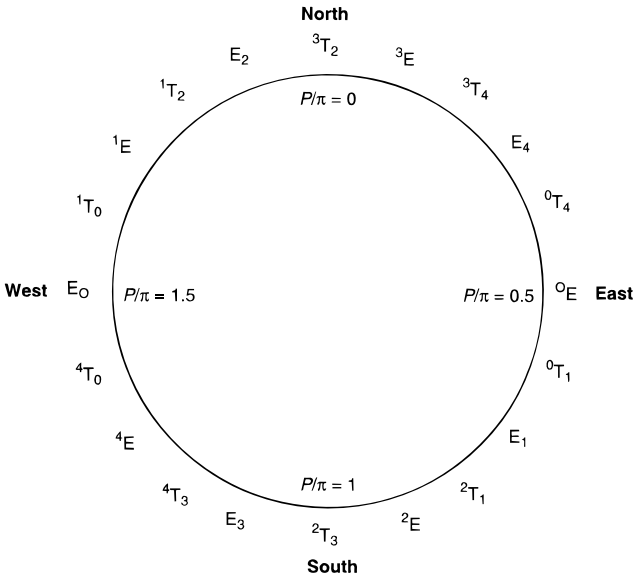

Pseudorotational wheel of a D-aldofuranosyl ring.

of the pseudorotational wheel (Scheme 2).[6,7] All possible E and T conformers are indicated at the perimeter of the circle organized such that those which are closely related to each other in structure are placed near each other. In solution, it is assumed that a given furanose ring exists as an equilibrating mixture of two conformations: one in the northern hemisphere and another in the southern hemisphere, respectively termed the north (N) and south (S) conformers, although generally one is favored. Rather than interconverting through inversion via a planar ring conformation in which all of the substituents are eclipsed, these conformers generally interconvert through pseudorotation.[7] For example, the ^3E and E_3 conformers could equilibrate through a series of twist and envelope conformations including either ^OE or E_O. The pathway by which two structures can interconvert (via the west or east) depends on the substituents on the ring.

A limited number of computational studies have attempted to address the problem of furanose ring conformation. Ma, Schaefer, and Allinger[8] have determined the energetic and conformational preferences of an array of furanoses at a variety of computational levels, including molecular mechanics (MM3), Hartree−Fock (HF/6-31G**), and density functional theory (B3LYP/6-31G**). In this same study, solvent effects were also included, using the IPCM reaction field model.[8] Psicose,[9] fructose,[10] sucrose,[11] and other fructofuranosyl oligomers[12] have been studied using molecular mechanics, and recently an ab initio treatment of the fructofuranose ring has been reported.[13]

Scheme 3

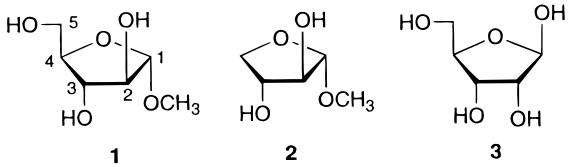

Serianni, Carmichael, and co-workers[14a−d] have studied the β-D-ribofuranosyl and 2-deoxy-β-D-ribofuranosyl rings at HF/6-31G* and MP2/6-31G* levels of theory. More recently, density functional theory (B3LYP/6-31G*) calculations of 2-deoxy-β-D-ribofuranose have been reported.[14e] Pérez, Imberty, and co-workers have investigated both α-L and β-D-arabinofuranosides at the MM3 level.[15] In some cases the computational efforts have been supported by solution NMR studies, and in particular for the D-fructofuranosyl, β-D-ribofuranosyl and 2-deoxy-β-D-ribofuranosyl rings, a detailed understanding of the conformational preferences is now available.[10−12,14] Finally, very recently the crystal structures of four pentofuranosyl methyl glycosides, namely methyl α-D-arabinofuranoside, methyl α-D-lyxofuranoside, methyl β-D-ribofuranoside, and methyl α-D-xylofuranoside, have been solved.[16] These crystal structures were in turn used as the starting points for geometry optimizations using a variety of levels of theory including MM3, HF/4-21G, HF/cc-pVDZ, B3LYP/4-21G, and B3LYP/cc-pVDZ.[16]

The core monosaccharide common to both the AG and LAM in mycobacteria is D-arabinofuranose. In these polymers, this sugar is found in both the α and β configuration, but the former is predominant. In conjunction with our ongoing work on the solution conformation of α-D-arabinofuranosyl oligosaccharides, we report here gas-phase ab initio and density functional theory calculations on the potential energy surface of methyl α-D-arabinofuranoside, **1** (Scheme 3).

Methods

Ab initio molecular orbital and density functional theory calculations were conducted using Gaussian 94.[17] Methyl α-D-arabinofuranoside, **1**, was studied at the Hartree−Fock (HF) and density functional theory (B3LYP) levels with the standard 6-31G* basis set. Ten envelope conformations (^3E, E_4, ^OE, E_1, ^2E, E_3, ^4E, E_O, ^1E, and E_2) and a planar structure were optimized using the method previously reported by Serianni and co-workers.[18] The protocol requires a specific endocyclic

(6) (a) Altona, C.; Sundaralingam, M. *J. Am. Chem. Soc.* **1972**, *94*, 8205. (b) Westhof, E.; Sundaralingam, M. *J. Am. Chem. Soc.* **1980**, *102*, 1493. (c) Harvey, S. C.; Prabhakaran, M. *J. Am. Chem. Soc.* **1986**, *108*, 6128. (d) Sundaralingam, M. *J. Am. Chem. Soc.* **1965**, *87*, 599.

(7) Westhof, E.; Sundaralingam, M. *J. Am. Chem. Soc.* **1983**, *105*, 970.

(8) Ma, B.; Schaefer, H. F., III; Allinger, N. L. *J. Am. Chem. Soc.* **1998**, *120*, 3411.

(9) French, A. D.; Dowd, M. K. *J. Comput. Chem.* **1994**, *15*, 561.

(10) French, A. D.; Dowd, M. K.; Reilly, P. J. *J. Mol. Struct. (THEOCHEM)* **1997**, *395−396*, 271.

(11) (a) French, A.; Schafer, L.; Newton, S. Q. *Carbohydr. Res.* **1993**, *239*, 51. (b) Cassett, F.; Imberty, A.; Hervé du Penhoat, C.; Koca, J.; Pérez, S. *J. Mol. Struct. (THEOCHEM)* **1997**, *395−396*, 211. (c) Tran, V.; Brady, J. W. *Biopolymers* **1990**, *29*, 961. (d) Tran, V. H.; Brady, J. W. *Biopolymers* **1990**, *29*, 977. (e) Hervé du Penhoat, C.; Imberty, A.; Roques, N.; Michon, V.; Mentech, J.; Descotes, G.; Pérez, S. *J. Am. Chem. Soc.* **1991**, *113*, 3720.

(12) (a) Waterhouse, A. L.; Horváth, K.; Liu, J. *Carbohydr. Res.* **1992**, *235*, 1. (b) Timmermans, J. W.; de Wit, D.; Tournois, H.; Leeflang, B. R.; Vliegenthart, J. F. G. *J. Carbohydr. Chem.* **1993**, *12*, 969.

(13) Chung-Phillips, A.; Chen, Y. Y. *J. Phys. Chem. A* **1999**, *103*, 953.

(14) (a) Podlasek, C. A.; Stripe, W. A.; Carmichael, I.; Shang, M.; Basu, B.; Serianni, A. S. *J. Am. Chem. Soc.* **1996**, *118*, 1413. (b) Church, T. J.; Carmichael, I.; Serianni, A. S. *J. Am. Chem. Soc.* **1997**, *119*, 8946. (c) Serianni, A. S.; Wu, J.; Carmichael, I. *J. Am. Chem. Soc.* **1995**, *117*, 8645. (d) Bandyopadhyay, T.; Wu, J.; Stripe, W. A.; Carmichael, I.; Serianni, A. S. *J. Am. Chem. Soc.* **1997**, *119*, 1737. (e) Cloran, F.; Carmichael, I.; Serianni, A. S. *J. Phys. Chem. A* **1999**, *103*, 3783.

(15) (a) Cros, S.; Hervé du Penhoat, C.; Pérez, S.; Imberty, A. *Carbohydr. Res.* **1993**, *248*, 81. (b) Cros, S.; Imberty, A.; Bouchemal, N.; Hervé du Penhoat, C.; Pérez, S. *Biopolymers* **1994**, *34*, 1433.

(16) Evdokimov, A. G.; Kalb (Gilboa), A. J.; Koetzle, T. F.; Klooster, W. T., Martin, J. M. L. *J. Phys. Chem. A* **1999**, *103*, 744.

(17) Frisch, M. J.; Trucks, G. W.; Schlegel, H. B.; Gill, P. M. W.; Johnson, B. G.; Robb, M. A.; Cheeseman, J. R.; Keith, T.; Petersson, G. A.; Montgomery, J. A.; Raghavachari, K.; Al-Laham, M. A.; Zakrzewski, V. G.; Ortiz, J. V.; Foresman, J. B.; Cioslowski, J.; Stefanov, B. B.; Nanayakkara, A.; Challacombe, M.; Peng, C. Y.; Ayala, P. Y.; Chen, W.; Wong, M. W.; Andres, J. L.; Replogle, E. S.; Gomperts, R.; Martin, R. L.; Fox, D. J.; Binkley, J. S.; Defrees, D. J.; Baker, J.; Stewart, J. P.; Head-Gordon, M.; Gonzalez, C.; Pople, J. A. *Gaussian 94, Revision D.3;* Gaussian, Inc.: Pittsburgh, PA, 1995.

(18) (a) Serianni, A. S.; Chipman, D. M. *J. Am. Chem. Soc.* **1987**, *109*, 5297. (b) Garrett, E. C.; Serianni, A. S. In *Computer Modeling of Carbohydrate Molecules:* French, A. D., Brady, J. W., Eds.; ACS Symposium Series 430; American Chemical Society: Washington, DC, 1990; pp 91−119. (c) Garrett, E. C.; Serianni, A. S. *Carbohydr. Res.* **1990**, *206*, 183.

Scheme 4

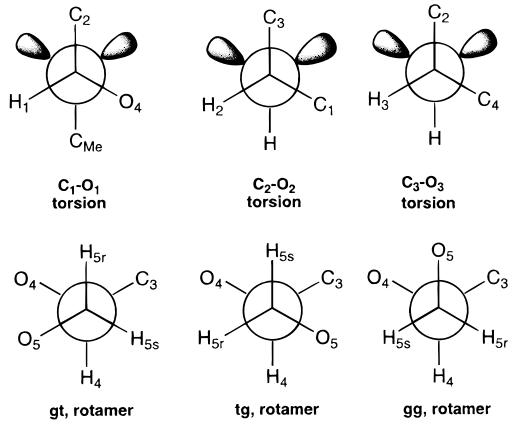

torsion angle to be constrained to 0° so that the conformation will be fixed in an envelope conformation. For example, the ^{O}E conformer was obtained by constraining the dihedral angle containing $C_4-C_3-C_2-C_1$ in a plane. The optimization was then carried out by leaving all other geometric parameters (such as bond distances, bond angles, and dihedral angles) to optimize completely. The planar structure was obtained via constriction of two endocyclic torsion angles (namely, $O_4-C_1-C_2-C_3$ and $C_4-O_4-C_1-C_2$) at 0°.[18]

The choice of exocyclic torsion angles was arbitrary except for the C_1-O_1 and C_5-C_4 bonds. The dihedral angle about the C_1-O_1 bond was initially chosen to maximize the *exo*-anomeric effect,[19] specifically the methyl group was placed antiperiplanar to the C_1-C_2 bond. For the C_5-C_4 bond, each of three staggered conformations, gg, gt, or tg (viewing down the C_5-C_4 bond axis), were explored (Scheme 4). As discussed in greater detail below, the specific rotamer about the C_5-C_4 bond present in each envelope has a significant effect on the conformer's ability to form intramolecular hydrogen bonds (H-bonds), which in turn profoundly influences its energy. Extensive work has been conducted on the gas-phase surface of pyranoses and their ability to form intramolecular H-bonds.[20] Extending this to the furanosyl surface (i.e., maximization of intramolecular H-bonds) also was used to limit the surface studied. This was necessary due to the fact that $3^5 \times 11 = 2673$ unique structures must be optimized for a full surface scan. Generation of such a surface is impractical with available computer resources. However, a number of starting geometries were used for each envelope conformation to ensure location of the true minimum energy structure.

The focus of this paper is to identify the torsional preferences about the five endocyclic bonds for each envelope. With this knowledge in hand, one should be able to remove the planar constraint and also include specific solvent molecules or dielectric fields for understanding the solution structure. Previous studies on carbohydrates with reaction field methods yielded mixed results,[8] and thus no attempt was made to include them in this current study.

The HF and B3LYP levels were chosen as a balance of expected computational time and accuracy. The lack of electron correlation in HF theory has been shown to raise the relative energies in some tetrafuranoses,[14c] and the B3LYP method has recently been applied to a number of furanosides.[8] Using the HF/6-31G* geometries, we have also explored further inclusion of electron correlation and extended basis sets at the HF, MP2, MP3 and B3LYP levels with the 6-31+G** basis set.[21]

(19) (a) Lemieux, R. U. *Pure Appl. Chem.* **1971**, *25*, 527. (b) Sulzner, U.; Schleyer, P. v. R. *J. Org. Chem.* **1994**, *59*, 2138.

(20) (a) Jebber, K. A.; Zhang, K.; Cassady, C. J.; Chung-Phillips, A. *J. Am. Chem. Soc.* **1996**, *118*, 10515. (b) Brown, J. W.; Wladkowski, B. D. *J. Am. Chem. Soc.* **1996**, *118*, 1190. (c) Barrows, S. E.; Dulles, F. J. *Carbohydr. Res.* **1995**, *276*, 219. (d) Csonka, G. I.; Éliás, K.; Csizmadia, I. G. *Chem. Phys. Lett.* **1996**, *257*, 49. (e) Cramer, C. J.; Truhlar, D. G. *J. Am. Chem. Soc.* **1993**, *115*, 5745. (f) Polavarapu, P. L.; Ewig, C. S. *J. Comput. Chem.* **1992**, *13*, 1255.

(21) Hehre, W. J.; Radom, L.; Schleyer, P. v. R.; Pople, J. A. *Ab initio Molecular Orbital Theory*; Wiley-Interscience: New York, 1986 and references therein.

Table 1. Energy Profile for Methyl α-D-Arabinofuranoside[a]

conformer	P/π	HF/6-31G*[b]	6-31+G**//HF/6-31G*[c] HF	MP2	MP3	B3LYP	B3LYP/6-31G*[b]
^{3}E	0.1	1.7	0.3	3.2	2.5	1.5	4.1
E_4	0.3	2.4	0.8	3.5	2.8	1.9	4.4
^{O}E	0.5	3.5	2.0	4.3	3.7	3.2	5.4
E_1	0.7	0.0	0.3	0.4	0.3	1.4	1.5
^{2}E	0.9	0.0	0.0	0.0	0.0	0.0	0.0
E_3	1.1	2.9	2.6	3.1	2.9	2.4	2.9
^{4}E	1.3	5.2	4.5	5.5	5.0	4.5	5.7
E_O	1.5	7.3	6.0	8.5	7.6	7.0	9.4
^{1}E	1.7	5.5	3.7	6.9	5.9	4.6	7.4
E_2	1.9	2.7	1.3	4.2	3.3	2.7	5.2
planar		8.0	6.7	9.5	8.5	6.9	9.3

[a] Relative energies are in kcal/mol at the bottom of the well. [b] Optimized geometry at the specified level. [c] Using the HF/6-31G* optimized geometries.

Results and Discussion

The calculations carried out for the 10 constrained envelopes and planar structure of **1** provided conformational energies and structural parameters (i.e., bond distances, bond angles, dihedral angles, and interatomic distances). The discussion which follows is a critical analysis of the effect of conformation on those parameters. In the discussion, P refers to the pseudorotational phase angle as previously defined.[6a]

Conformational Energy Profile. As illustrated in Table 1 and Figure 1, ring conformation is intimately related to the relative energy. On the optimized HF/6-31G* hypersurface, E_1 ($P/\pi = 0.7$) is the global minimum, but is only 0.04 kcal/mol more stable than ^{2}E ($P/\pi = 0.9$). However, at the optimized B3LYP/6-31G* level, ^{2}E is 1.5 kcal/mol more stable than E_1. These results are in contrast to those of Serianni on β-D-ribofuranose[14] which demonstrated that the use of electron correlation at the MP2/6-31G* level gave energies *lower* than those obtained at HF. The local minimum in the northern hemisphere is the same regardless of the level of theory (Figure 1A), namely ^{3}E ($P/\pi = 0.1$). Relative to the global minimum, the ^{3}E conformer is destabilized by 1.7 kcal/mol (HF) or 4.1 kcal/mol (B3LYP).

We have explored the effect of including electron correlation on the relative energies at the MP2, MP3 and B3LYP levels with the 6-31+G** basis set and the HF/6-31G* geometries. These results are shown in Figure 1B. The qualitative results are the same for all of these theoretical levels and even the HF/6-31+G**//HF/6-31G* level predicts that E_1 is less stable than ^{2}E. In general, the MP3 and B3LYP results are in reasonable agreement. Also, the qualitative trends of the fully optimized (with ring constraint) energies are similar to the single-point energies.

Conversion between the global minimum and other local minima can either occur through pseudorotation via an eastern or western route or by inversion through the planar ring form.[5,7] At both (optimized) HF/6-31G* and B3LYP/6-31G* levels of theory, our calculations show that the eastern pathway is the energetically preferred route. Pseudorotation through the east requires that the ring traverse through the ^{O}E ($P/\pi = 0.5$) conformation which is 3.5 kcal/mol (HF) or 5.4 kcal/mol (B3LYP) higher in energy than the global minimum. In contrast, pseudorotation through the west must necessarily involve the E_O ($P/\pi = 1.5$) conformer which is 7.3 kcal/mol higher in energy than the global minimum (HF). In our B3LYP calculations, we find that the E_O conformer is 9.4 kcal/mol higher in energy than the global minimum.

Previous computational investigations of furanose rings have demonstrated that inversion through the planar conformer is the

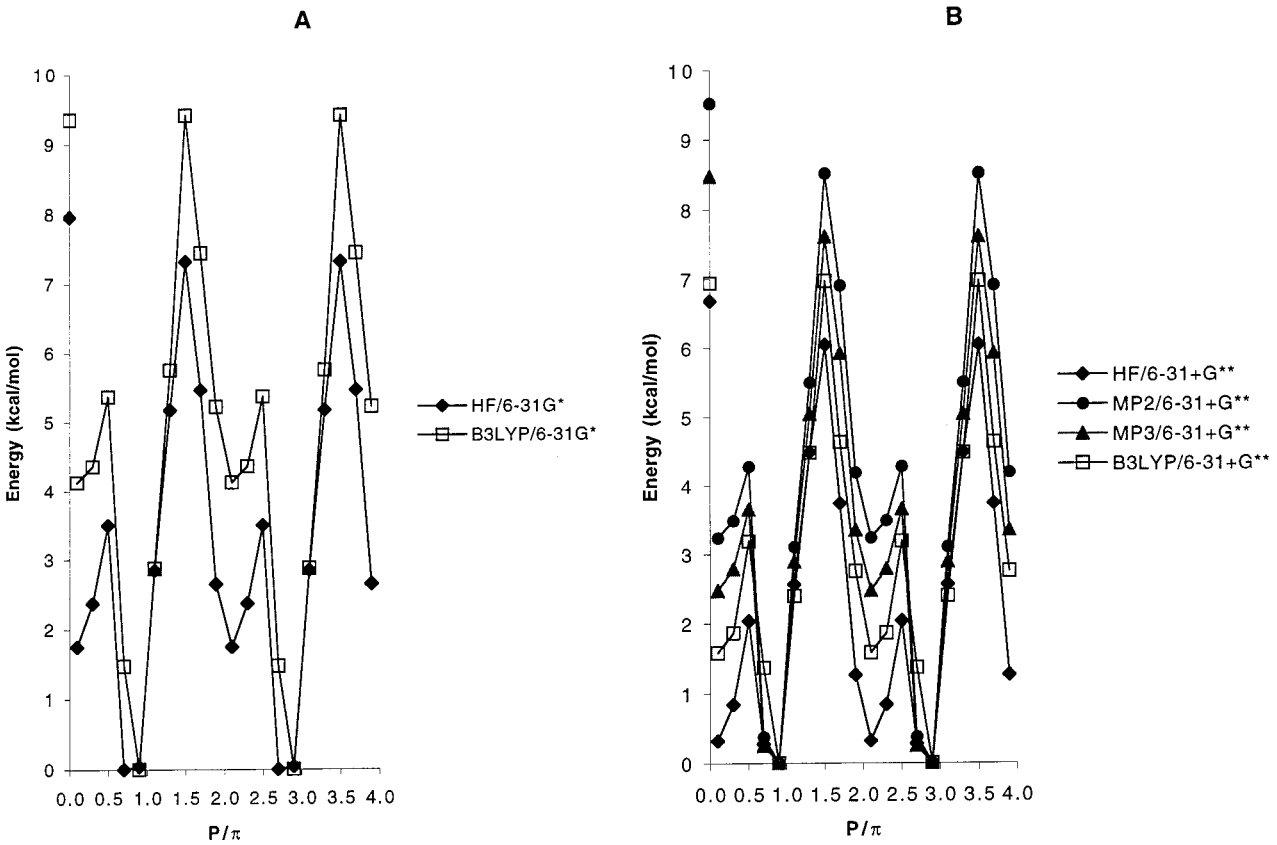

Figure 1. Energy profile of **1** for the 10 envelope conformations at (A) HF/6-31G* and B3LYP/6-31G* and (B) extended basis set calculations based on HF/6-31G* single points. The energies of the planar conformer are placed on the *y* axis. One cycle is $0-2$ P/π (radians), where 0.1 $P/\pi = {}^3E$ (See Scheme 2).

least favorable pathway for interconversion between conformers,[7,14a] due to eclipsing of all exocyclic bonds. For example, in β-D-ribofuranose (**3**), the planar conformer was calculated (HF/6-31G*) to be 6.5 kcal/mol higher in energy than the global minimum.[14a] In contrast, the energy barrier through pseudorotation was 3.7 kcal/mol (east pathway) or 4.4 kcal/mol (west pathway). We were therefore surprised to discover that for the conformations of **1**, the energy difference between the planar form and the highest energy envelope conformer (E_O) was small. At the HF level of theory, the E_O conformer has an energy of 7.3 kcal/mol and the planar form is 8.0 kcal/mol. Thus, while the inversion pathway is still less favorable than pseudorotation through the west, the energy barriers are comparable. When the B3LYP/6-31G* level is used for these calculations, the planar form (9.3 kcal/mol) was found to be slightly *more* stable than the E_O conformer (9.4 kcal/mol). These results suggest that for **1**, conformer equilibration through the planar ring form is a viable alternative to pseudorotation through the west. It should, however, be emphasized that either pathway is not expected to contribute as the barrier to pseudorotation through the east is significantly (4.9 kcal/mol) smaller than either inversion or pseudorotation through the west. Illustrated in Figure 2 are the five envelope conformers that are involved in pseudorotation through the eastern pathway.

When one considers the stereochemistry of the α-D-arabinofuranosyl ring (**1**), it is perhaps understandable that in comparison to the β-D-ribofuranosyl ring (**3**), the energy of the planar form is more comparable to the high-energy envelope conformers. All of the ring substituents on the α-D-arabinofuranosyl ring are *trans;* whereas, in the *ribo*-isomer the substituents at C_2 and C_3 are *cis* to each other. It would be anticipated that for the latter ring system, the eclipsing interactions present in the planar form would be more severe. A similar observation has been made previously in HF/6-31G* calculations on α-D-threofuranose, **2**. In this monosaccharide, which has the same stereochemistry as **1** at the C_1, C_2, and C_3 positions, the planar ring form has been calculated to be of comparable energy to the highest-energy envelope conformation.[17a]

A final feature which greatly effects the energy profile is the torsion angle about the C_5-C_4 bond. Three possible staggered conformations (gg, gt, or tg) about this bond are possible (Scheme 4). All envelopes show a preference for the gg rotamer, except ${}^1E$ ($P/\pi = 1.7$) in which the C_5-C_4 bond is in the gt conformation. For all envelopes, when the initial torsion angle about this bond was set in the tg conformation, the structure minimized to either the gt or gg conformation. On the other hand, when the initial torsion was set at either gg or gt, minimization resulted in no change in the rotamer. For the envelopes on this surface, which differed only in the rotamer about C_5-C_4 bond, the gg rotamer was typically 0.5 to 3.0 kcal/mol more stable than either the gt or tg rotamers.

The stability trend is, in part, related to the ability of these rotamers to form intramolecular H-bonds. In the gg rotamer, the hydroxyl group at C_5 (OH_5) can potentially serve as either an H-bond acceptor or donor with the hydroxyl group on C_2 (OH_2), or as an H-bond donor to the ring oxygen (O_4). In the gt rotamer, the OH_5 group can act only as an H-bond donor to the ring oxygen. Finally, in the tg rotamer, the OH_5 group can either accept or donate a hydrogen to generate an H-bond with the hydroxyl group on C_3 (OH_3); however, in many conformers the distance between these groups is too long for efficient H-bonding to occur. In Table 2, the intramolecular H-bonding interactions present in the different conformations of **1** are shown. In many, but not all, of these envelopes, H-bonds are

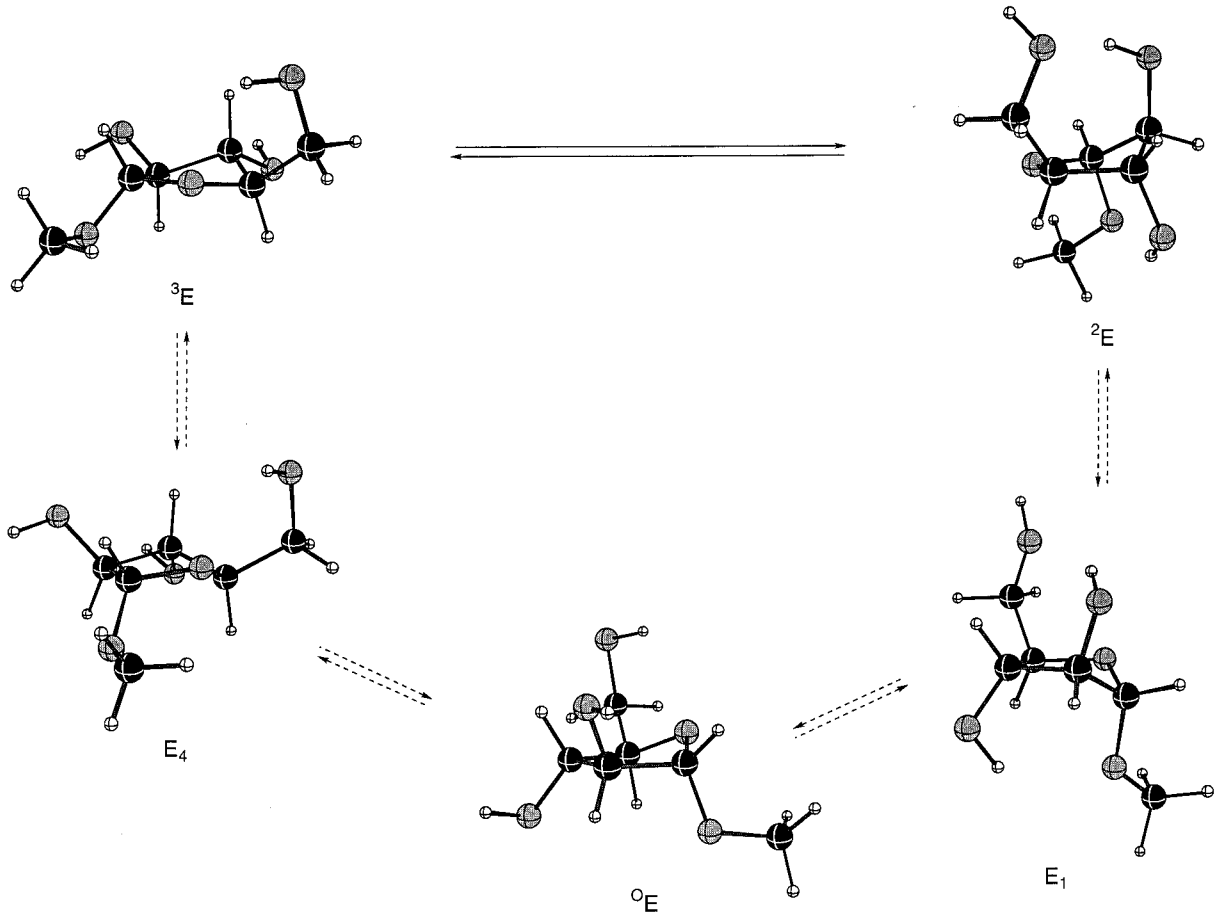

Figure 2. Conformers present along the (preferred) eastern pseudorotational pathway for **1**. Conformers shown are those obtained from the B3LYP/6-31G* calculations.

Table 2. Intramolecular Hydrogen Bonding[a]

con-former	P/π	type[b]	HF/6-31G* distance	HF/6-31G* angle	B3LYP/6-31G* distance	B3LYP/6-31G* angle
^{3}E	0.1	$OH_5\cdots O_4$	2.39	103.7	2.29	110.0
E$_4$	0.3	$OH_5\cdots O_4$	2.38	104.6	2.30	109.8
^{O}E	0.5	$OH_5\cdots O_4$	2.38	105.5	2.31	110.3
E$_1$	0.7	$OH_5\cdots O_4$	2.41	106.4	2.35	110.2
		$OH_3\cdots O_1$	2.43	124.7	2.35	128.7
^{2}E	0.9	$OH_3\cdots O_1$	2.22	132.9	2.08	138.3
		$OH_2\cdots O_5$	1.91	155.7	1.82	158.1
E$_3$	1.1	$OH_3\cdots O_1$	2.53	130.2	2.36	136.0
		$OH_2\cdots O_5$	1.90	152.3	1.81	157.1
^{4}E	1.3	$OH_2\cdots O_5$	2.03	144.3	1.92	148.9
E$_O$	1.5	$OH_2\cdots O_5$	2.60	131.4	2.52	134.4
^{1}E	1.7	$OH_5\cdots O_4$	2.37	107.8	2.28	112.4
E$_2$	1.9	$OH_5\cdots O_4$	2.46	100.0	2.35	106.9

[a] Distances are in angstroms and angles are in degrees. [b] Hydrogen bond defined as the hydrogen donor···oxygen acceptor.

formed between OH_5 and O_4 (designated as an $OH_5\cdots O_4$ H-bond). However, the data suggest that, as discussed in greater detail below, if O_5 can act as an H-bond acceptor from OH_2 (designated as an $OH_2\cdots O_5$ H-bond), then it will do so in preference to H-bonding to the ring oxygen. As is clear from Table 2, the H-bonds formed between OH_5 and the ring oxygen O_4 would be anticipated to be relatively weak as the angle average is 104.7° at HF/6-31G* and 109.9° at B3LYP/6-31G*, far from the ideal linear geometry for a H-bond.[22] In addition to intramolecular H-bonding, it is likely that the gg and gt conformers are also stabilized by the *gauche* effect.[23] In both of these conformations, O_4 and O_5 are *gauche* to each other, whereas these same oxygens are *trans* in the tg form.

In only one envelope conformer (^{1}E, $P/\pi = 1.7$) is the gt rotamer energetically preferred over the gg rotamer. The energy difference between these two conformations is 0.5 kcal/mol (HF) or 1.6 kcal/mol (B3LYP), emphasizing that H-bonds are poorly represented at the HF level.[24] In both the gg and gt rotamers the values of the $OH_5\cdots O_4$ distance and H-bonding angle are comparable at the B3LYP level. However, the ^{1}E gg conformer on the HF surface does not have any $OH_5\cdots O_4$ stability as the distance between the H and O_4 is 2.69 Å and the angle made for the bond is 91.4°.

Recently, MM3, HF/4-21G, HF/cc-pVDZ, B3LYP/4-21G, and B3LYP/cc-pVDZ calculations on **1** have been reported.[16] In that study, the geometry present in the crystal structure (E$_4$, $P/\pi = 0.3$, see below) was taken and further optimized without the planar constraint used in our investigations. In all cases except HF/4-21G, these calculations identified a local minimum at E$_4$. When a comparison was made between various structural parameters in the gas-phase and crystalline geometries, the best agreement was observed in the B3LYP/cc-pVDZ optimizations (see the table in Supporting Information). These results are in general agreement with ours in which we have identified a local minima at ^{3}E, the envelope conformer immediately adjacent to E$_4$. As indicated in Table 1, the energy differences between these two conformers is small: 0.7 kcal/mol (HF) and 0.3 kcal/mol (B3LYP), and the apparent discrepancy could be related to the different basis sets used.

(22) Jeffrey, G. A. *An Introduction to Hydrogen Bonding*; Oxford Press: New York, 1997; pp 11−32.

(23) Wolfe, S. *Acc. Chem. Res.* **1972**, *5*, 102.

(24) Wiberg, K. B.; Hadad, C. M.; LePage, T. J.; Breneman, C. M.; Frisch, M. J. *J. Phys. Chem.* **1992**, *96*, 671.

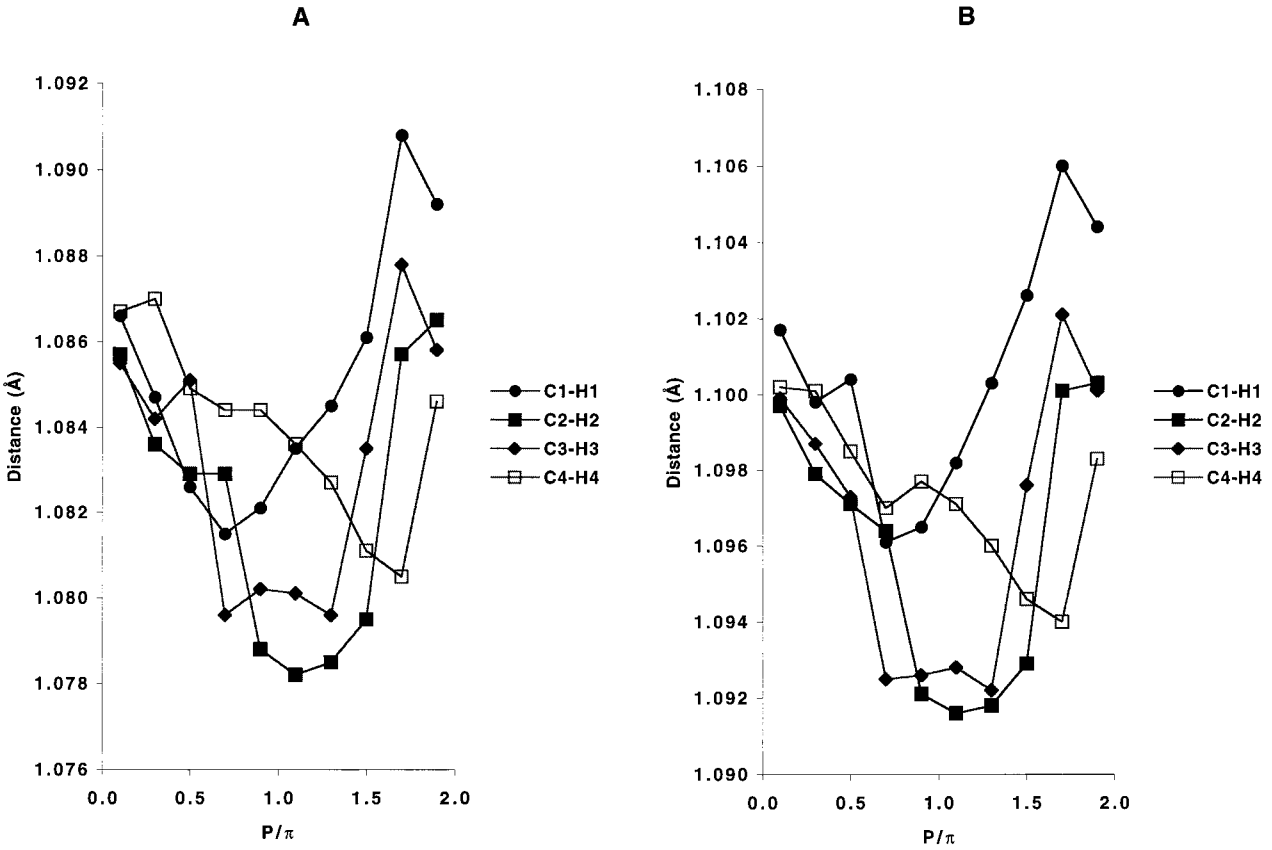

Figure 3. The dependence of C−H exocyclic bond distances on ring conformation of **1** at (A) HF/6-31G* and (B) B3LYP/6-31G*.

Extended basis set calculations and electron correlation using the HF/6-31G* geometries provide an energy profile almost identical to that obtained from the optimized geometry calculations. B3LYP/6-31+G**, MP2/6-31+G**, MP3/6-31+G**, and HF/6-31+G** single-point energies that were obtained confirm that the E_1 point on the HF/6-31G* surface is an artifact of the smaller basis set.

Bond Lengths. The relationship between C−H bond distances and ring conformation in ribofuranosides has been detailed by Serianni and others[14,18] and is dependent upon whether the bond is pseudoaxial (longer) or pseudoequatorial (shorter). Our calculations show that for **1**, a similar trend is observed for the C_1-H_1, C_2-H_2, C_3-H_3, and C_4-H_4 bonds at both levels of theory (Figure 3). Conformations in which a particular C−H bond is pseudoaxial have C−H bonds that are longer than those in which the same bond is pseudoequatorial (e.g., the C_1-H_1 bond in the ^{1}E conformer is longer than in E_1).

The exocyclic C−O and C−C bond lengths have been shown to be sensitive to the conformation in other furanose rings.[14a,18] In **1**, three of these bond lengths (C_2-O_2, C_3-O_3, and C_4-C_5) do not vary appreciably as a function of conformation (see Supporting Information for the graph). However, as expected, to optimize the *endo*-anomeric effect, the C_1-O_1 bond length is at a maximum at ^{2}E (pseudoaxial C_1-O_1 bond) and a minimum at ^{1}E (pseudoequatorial C_1-O_1 bond) at the HF and B3LYP levels (Figure 4).

The endocyclic C−O and C−C bonds vary in a manner similar to the β-D-ribofuranosyl ring.[14] As illustrated in Figure 4, the length of the C_1-O_4 bond is shorter in conformations when C_1-O_1 is pseudoaxial (e.g. ^{2}E) as would be expected due to the *endo*-anomeric effect. The length of the C_4-O_4 bond is also sensitive to conformation but we are unable to rationalize the observed trend; similar results have been demonstrated for the β-D-ribofuranosyl ring.[14c] In general, the length of the C_4-O_4 bond is at a minimum in conformations where the ring oxygen is out of the plane (^{O}E and E_O).

The distances of the endocyclic C−C bonds are shown in Figure 5 and are sensitive to ring conformation. The C−C endocyclic bond distances are maximum in conformers in which the bond is in the plane of the envelope, and opposite to the out-of-plane atom (e.g., the C_2-C_3 bond in ^{O}E and E_O). A possible explanation for this behavior is that the increase in length minimizes the steric repulsion between the exocyclic groups (e.g., OH) attached to these bonds, which will be essentially eclipsed. The minima, which occur where one of the atoms of the bond is either above or below the plane of the ring, are less readily explained.

C−O Bond Dihedral Angles. The 10 envelopes of **1** provided interesting results with respect to the three exocyclic C−O bond dihedral angles (Figure 6). As expected, the C_1-O_1 bond dihedral angle ($O_4-C_1-O_1-C_{Me}$) was insensitive to the ring conformation. The value of this angle varies between 63 and 68° (HF) and 63 and 70° (B3LYP), and the preference for the orientation about this bond is a result of the *exo*-anomeric effect, which necessitates that one of the lone pairs on O_1 be aligned antiperiplanar to the C_1-O_4 bond. On the other hand, the $H_2-C_2-O_2-H$ and $H_3-C_3-O_3-H$ torsion angles do change appreciably with conformation. The torsion angles for these bonds approach 180° in conformations where intramolecular H-bonding is possible and 60° in those conformations where these H-bonding interactions are not possible. For example, in the ^{2}E conformer ($P/\pi = 0.9$), OH_2 and OH_5 are close enough to effectively H-bond (Table 2) which causes the $H_2-C_2-O_2-H$ dihedral angle to approach 180°. On the other hand, in the ^{O}E conformer ($P/\pi = 0.5$), these same groups are too distant to form an effective H-bond. In this case, the dihedral angle is close to 50°. It should be noted that H-bonds between OH_2 and

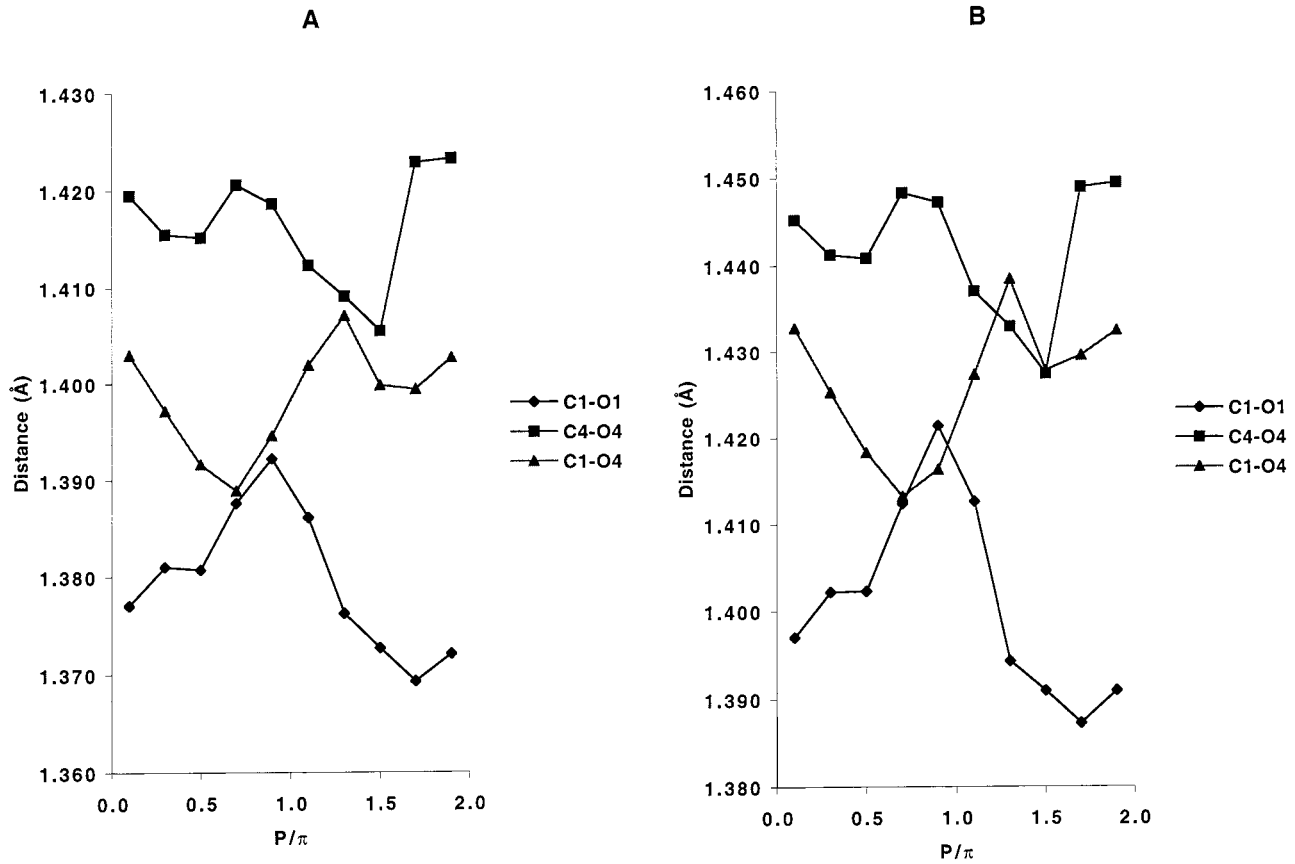

Figure 4. The dependence of C−O exocyclic bond distances on ring conformation of **1** at (A) HF/6-31G* and (B) B3LYP/6-31G*.

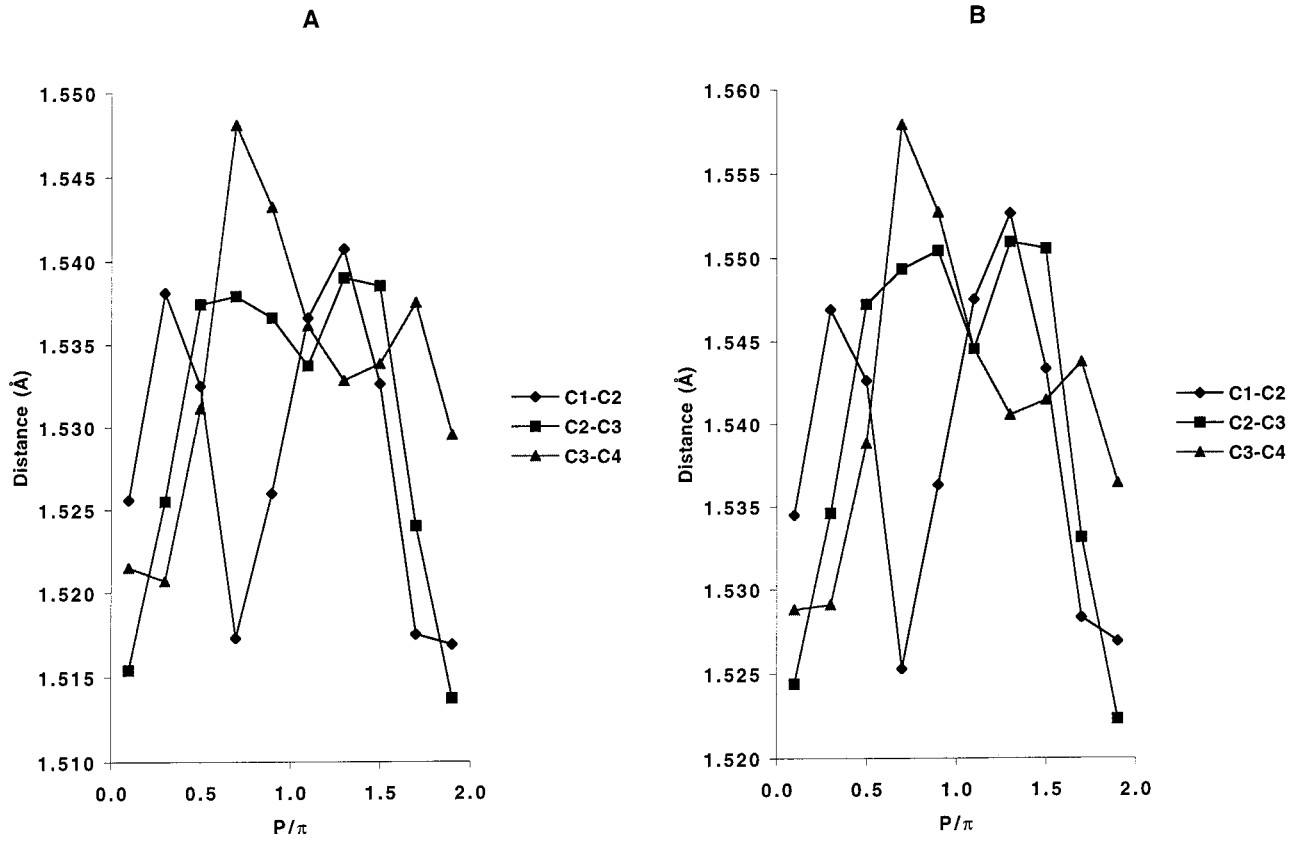

Figure 5. The dependence of C−C exocyclic bond distances on ring conformation of **1** at (A) HF/6-31G* and (B) B3LYP/6-31G*.

OH_5 always form such that the latter is the H-bond donor and the former the H-bond acceptor; the converse is never observed. In addition, intramolecular H-bonding between groups oriented 1,3-*cis* on the ring is not limited to the hydroxyl groups at C_2 and C_5. In the E_1 ($P/\pi = 0.7$), ^2E ($P/\pi = 0.9$), and E_3 ($P/\pi = 1.1$) conformers, the C_3 hydroxyl group acts as an H-bond donor

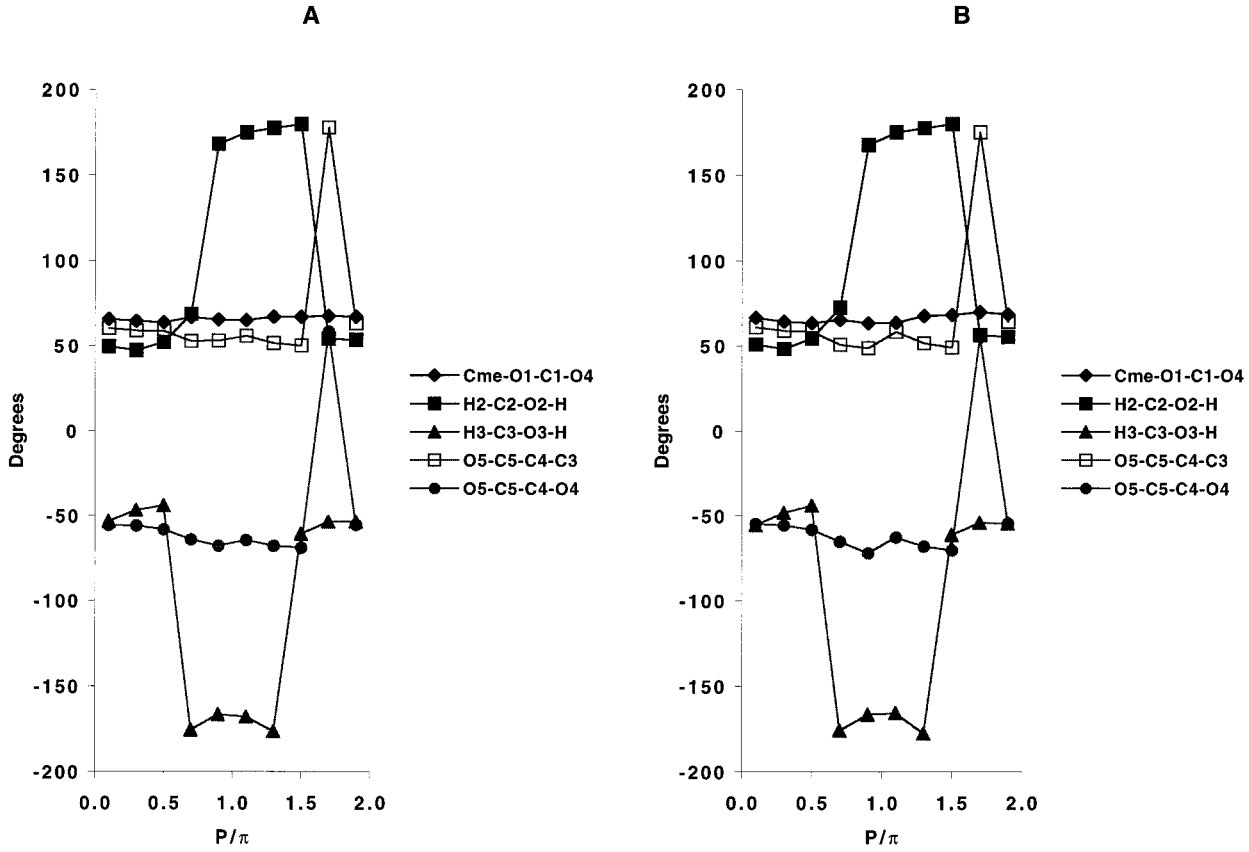

Figure 6. The dependence of C−O dihedral angles as a function of ring conformation of **1** at (A) HF/6-31G* and (B) B3LYP/6-31G*.

to O_1. It is important to mention that two of the three most stable conformers (^{2}E, E_1, and E_3 at B3LYP) all possess both $OH_2\cdots O_5$ and/or $OH_3\cdots O_1$ H-bonds. This is in agreement with previous work that suggested the important role that intramolecular H-bonds play in stabilizing carbohydrates in the gas phase.[8,19,25] In the two most stable conformations, no $OH_5\cdots O_4$ H-bonds are seen which suggests that any stabilization gained by this interaction is relatively small.

Exocyclic Dihedral Angles. Four dihedral angles involving exocylic groups ($O_1-C_1-C_2-O_2$, $O_2-C_2-C_3-O_3$, $O_3-C_3-C_4-O_4$, and $O_3-C_3-C_4-C_5$) are all sensitive to ring conformation, and the values of these angles are also an indicator of the ability of the conformer to form intramolecular H-bonds (Figure 7). In those conformers which possess extensive intramolecular H-bonding, the oxygens are oriented in a pseudoaxial fashion. Given the 1,2-*trans* relationship between the exocyclic oxygens, an increase in the dihedral angle between these groups is driven by their ability to participate in H-bonding interactions. Only one dihedral angle ($O_4-C_4-C_5-O_5$) is insensitive to conformation. This is to be expected because, as discussed previously, in all conformers, the favored rotamer about the C_4-C_5 bond in all but one of the conformers is gg, and as a consequence the $O_4-C_4-C_5-O_5$ dihedral angle is independent of the ring conformation.

Shown in Figure 8 are the intracyclic H,H dihedral angles as a function of conformation. As expected three of these angles ($H_1-C_1-C_2-H_2$, $H_2-C_2-C_3-H_3$, and $H_3-C_3-C_4-H_4$) are sensitive to conformation. The portion of the pseudorotational itinerary between the north and south conformers (^{3}E and ^{2}E, respectively) is of particular importance as these dihedral angles are strongly related to the conformation in this region. This suggests that ^{1}H,^{1}H NMR coupling constants, which are intimately related to H,H dihedral angles, will be sensitive to conformation, and the use of experimentally observed couplings can be effectively used in PSEUROT calculations[26] for determining the relative ratio of equilibrating conformers.

The internuclear distances between protons are in some cases sensitive to conformation. Those involving only 1,2-hydrogens on the ring vary in a parabolic fashion between 2.8 and 3.0 Å. The distance between the 1,3-hydrogens, such as H_1-H_3 and H_2-H_4, are more sensitive to conformation, varying by more than 1 Å across the pseudorotational itinerary (see Supporting Information for the graphs).

Ring Puckering. The degree of displacement from the plane of the out-of-plane atom is illustrated in Figure 9 and varies by more than 10° (15−26°) across the pseudorotational itinerary. The largest puckering angle is found in one of the most stable conformers, E_1 ($P/\pi = 0.7$). This may arise as a consequence of the desire of OH_2 to form an intramolecular H-bond with O_5. Increasing the displacement of C_1 from the plane of the envelope would in turn decrease the distance between OH_2 and O_5, thus facilitating the H-bonding. The smallest extent of ring puckering is found in the highest-energy conformer, E_O ($P/\pi = 1.5$). The trend toward planarity in this conformer may be the result of the fact that this conformation is destabilized by the lack of *endo*-anomeric effect and the placement of the hydroxymethyl group pseudoaxial. Flattening of the ring would be expected to not only move the hydroxymethyl group to a less pseudoaxially oriented (more stable) position but would also allow for more anomeric stabilization by placing the glycosidic oxygen in a more pseudoaxial orientation. However,

(25) (a) Petrová, P.; Koca, J.; Imberty, A. *J. Am. Chem. Soc.* **1999**, *121*, 5535. (b) Whitfiled, D. M. *J. Mol. Struct. (THEOCHEM)* **1997**, *395*−*396*, 53.

(26) (a) PSEUROT 6.2; Gorlaeus Laboratories: University of Leiden. (b) de Leeuw, F. A. A. M.; Altona, C. *J. Comput. Chem.* **1983**, *4*, 428.

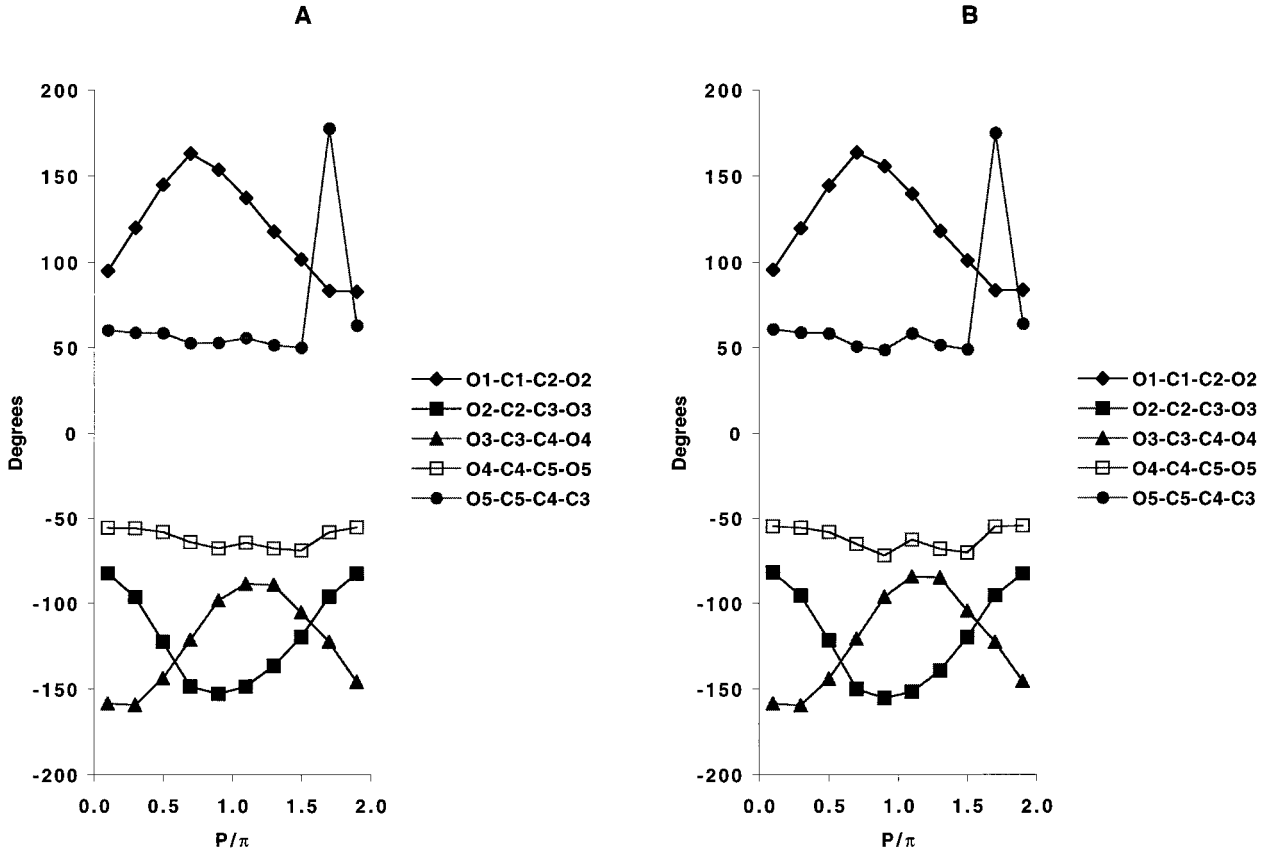

Figure 7. The dependence of O_x-O_y dihedral angle on ring conformation of **1** at (A) HF/6-31G* and (B) B3LYP/6-31G*.

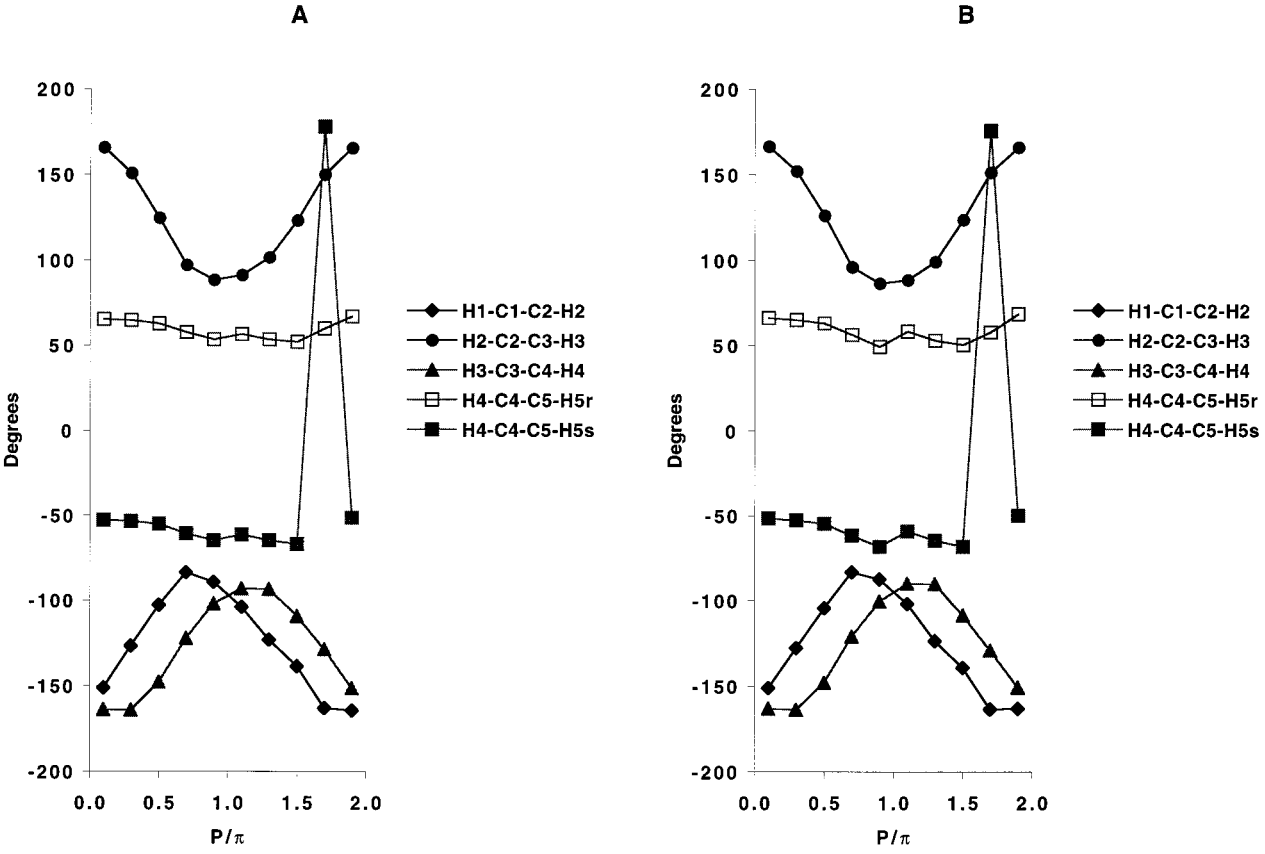

Figure 8. The dependence of H_x-H_y dihedral angle on ring conformation of **1** at (A) HF/6-31G* and (B) B3LYP/6-31G*.

it should also be appreciated that as the ring becomes more planar, eclipsing interactions between ring substituents will also increase. Therefore, in this conformer there appears to be a balance between these competing destabilizing factors. A similar

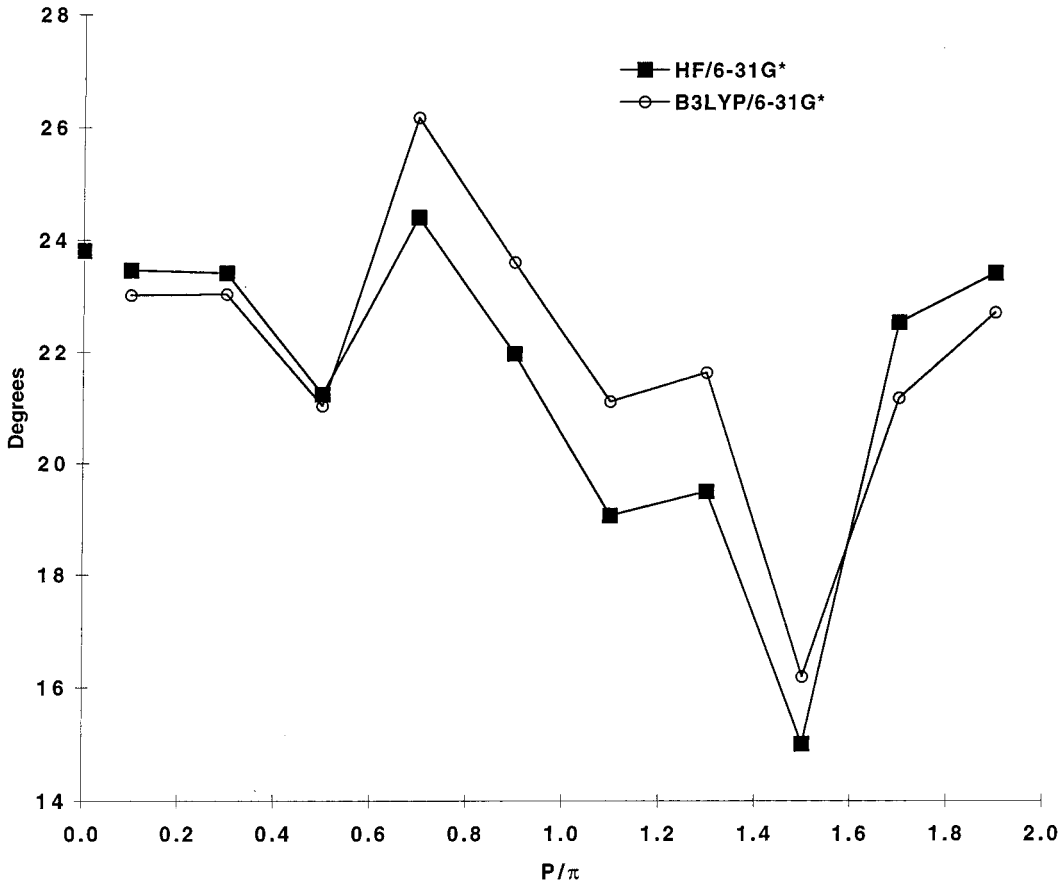

Figure 9. The effect of the ring puckering as a function of ring conformation of **1** at HF/6-31G* (■) and B3LYP/6-31G* (○). The puckering of the furanose ring in the crystal structure of **1** is placed on the *y* axis.

trend is observed for β-D-ribofuranose (**3**); in this sugar the E_O conformer is the least puckered of all the conformers.[14a] However, for **3** it was proposed that the decrease in puckering was solely the result of steric effects due to the *cis* orientation of the groups at C_1 and C_4.

The magnitudes of the ring puckering are consistent with the crystal structure of methyl α-D-arabinofuranoside (**1**),[16] In the crystal, the unit cell is comprised of two distinct structures that are almost identical. The ring in both unit cell molecule adopts an E_4 ($P/\pi = 0.3$) conformation with C_4 being 24.2° out of the plane. This displacement is virtually identical with the ring puckering calculated at both levels of theory for the E_4 conformer and provides further support that the molecular parameters obtained from these calculations are accurate. Furthermore, comparison of the bond angles, bond lengths, and torsion angles present in the crystal structure of **1** with those reported here for the E_4 conformer show excellent agreement. Additionally, the values of these structural parameters (see Supporting Information for table) obtained from our B3LYP/6-31G* calculations are very similar (and in some cases identical) to those calculated using B3LYP/cc-pVDZ,[16] suggesting that either basis set could be used for obtaining the geometry of this system.

Conclusions

This investigation was carried out in order to determine the conformational preferences of the α-D-arabinofuranosyl ring and the relationship between conformation and various structural parameters. The material presented here will be of great use in understanding the solution conformation of oligosaccharides containing α-D-arabinofuranosyl residues, which are found in two mycobacterial cell wall polysaccharides. The notable features reported in this study can be summarized as follows:

(a) Our computational study of **1** identifies the ^2E conformer at the B3LYP level as the most stable, and the HF level predicts that the ^2E and E_1 are almost degenerate. Both are found in the southern hemisphere of the pseudorotational itinerary. Further inclusion of electron correlation predicts that ^2E is the most stable conformer. The northern minimum was the ^3E conformer, which was either 1.7 or 4.1 kcal/mol less stable than the global minimum, depending on the level of theory. The computed energy profile shows that the conformers lying in the eastern hemisphere are considerably more stable than those in the western hemisphere, and therefore pseudorotation through the eastern hemisphere will be preferred.

(b) At the HF level of theory, the planar ring form is of higher energy than all of the envelope conformations. However, the B3LYP calculations show that the planar structure is of slightly lower energy than the E_O conformer. For the low energy ring conformers to equilibrate by pseudorotation through the western hemisphere, the ring must at some point adopt the E_O conformation, and this study suggests that inversion though the planar ring form may be a viable alternative pathway. This is in contrast to previous calculations[14] on the β-D-ribofuranosyl ring where it was concluded that pseudorotation through either the eastern or western hemisphere is preferred to inversion through the planar form.

(c) The HF and B3LYP calculations provide qualitatively similar trends, especially for the energy profile, but the absolute and relative energies are different. This is a significant benefit to the computational chemist when one considers the quality of answer obtained for the computer expense. MP2/6-31G*

calculations on β-D-ribofuranose suggest that electron correlation gave lower relative energies than at the HF level, but similar qualitative trends. We observe consistent trends between the HF/6-31G* and the B3LYP/6-31G* optimized geometries, and the relative trends at the B3LYP level is in reasonable agreement with the other electron correlation methods. Because of this finding and the success obtained for a reasonable amount of computer time, we recommend that the B3LYP/6-31G* level can be used effectively for these calculations. Similar findings have recently been reported for 2-deoxy β-D-ribofuranose.[14e]

The use of extended basis set calculations on the HF/6-31G* geometries indicate that electron correlation yields qualitatively similar trends; however, the energies obtained are uniformly higher than those of HF theory.

(d) The torsional parameters outlined herein lead to the conclusion that intramolecular H-bonding of polyols is a significant feature leading to the stabilization of these molecules in the gas phase. Ma, Schaefer, and Allinger's[8] on the potential energy surfaces and equilibrium populations of the D-aldo- and D-ketohexoses also supports this correlation as does other previous computational work on carbohydrates in the gas-phase.[20,25] Unquestionably, the effect of solvation on these intramolecular H-bonding patterns (as well as the overall energies) will be profound.

(e) A number of structural parameters are, as expected, sensitive to conformation. In particular, in the region of the pseudorotational itinerary expected to be populated at equilibrium, H,H dihedral angles are related to conformation. This bodes well for the use of three-bond H,H spin couplings in PSEUROT[26] calculations for assessing equilibrium populations of ring conformers.

We are currently exploring removing the torsional constraint, as well as the use of explicit solvent molecules or dielectric field effects on the potential energy surfaces, and these studies will be reported in due course.

Acknowledgment. This research has been supported by The Ohio State University and the National Science Foundation (T.L.L.: CHE-9875163 and C.M.H.: CHE-9733457). We acknowledge support from the Ohio Supercomputer Center where some of these calculations were performed.

Supporting Information Available: Cartesian coordinates for optimized structures, absolute energies, trend lines for all parameters not provided in the text, and a table comparing structural parameters calculated by us with work reported in ref 16 (PDF). This material is available free of charge via the Internet at http://pubs.acs.org.

JA9915091